

Creating, Preserving, and Directing Carboxylate Radicals in Ni-Catalyzed C(sp³)–H Acyloxylation of Ethers, Ketones, and Alkanes with Diacyl Peroxides

Vera A. Vil', Yana A. Barsegyan, Leah Kuhn, Alexander O. Terent'ev,* and Igor V. Alabugin*



Cite This: <https://doi.org/10.1021/acs.organomet.2c00663>



Read Online

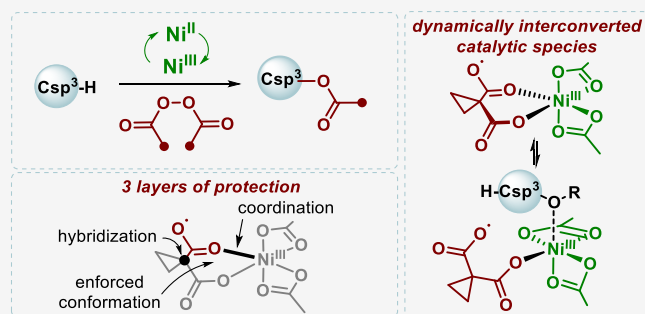
ACCESS |

Metrics & More

Article Recommendations

Supporting Information

ABSTRACT: The reaction of Ni(II) acetate with diacyl peroxides produces high-valence Ni-species capable of catalytic oxidative acyloxylation of C(sp³)–H bonds in ethers, ketones, and alkanes. The desired esters were obtained in 20–82% yields. Computational analysis suggests that activation of the peroxide moiety produces a dynamically interconverting mixture of catalytic Ni-species in the formal Ni(III) state. Remarkably, in these species, coordination of the RCO₂ group at Ni preserves radical character at the carboxylate moiety (i.e., carboxylate radical acts as an “L-ligand”), so the latter can induce fast C–H abstraction. The spirocyclopropyl moiety prevents premature radical decarboxylation via a combination of hybridization factors and stereoelectronic effects. A variety of viable C–H activation patterns were identified experimentally and computationally.



INTRODUCTION

Nickel-catalyzed functionalization of C–H bonds is gaining popularity as a powerful approach to forming new carbon–carbon and carbon–heteroatom bonds.^{1–3} Nickel is a low-cost alternative to precious metals with the ability to participate in both one- and two-electron redox processes. As a result, Ni can enable functionalization pathways complementary to the Pd-based catalytic systems.^{4–6} In particular, a number of recent studies illustrate that high-valent Ni(III) and Ni(IV) species open access to novel cross-coupling processes and unprecedented transformations.^{7–15}

Traditionally, oxidative functionalization involving peroxide oxidants are mediated by copper, iron, cobalt, or manganese compounds.¹⁶ Historically, the first example of such transformation was the Kharasch–Sosnovsky reaction.¹⁷ In this approach a transition metal/peroxide combination was used for the acyloxylation via C–H activation (Scheme 1A).

The potential of Ni-catalyzed oxidative C–H functionalization^{18,19} is underexplored in comparison to both precious metals (Pd, Au, Ru, Ir) and other earth-abundant metals (Cu, Fe, Co). In general, high-valent nickel complexes are considerably unstable so the Ni(II)/Ni(III) cycle in oxidative processes with peroxides is more difficult to achieve than the corresponding cycles of Cu(I)/Cu(II), Fe(II)/Fe(III), and Mn(II)/Mn(III).

Until recently, nickel/peroxide systems have been only used in a few oxygen transfer processes.^{20–24} In 2016, the Chatani group reported dicumyl peroxide as a methyl source for the Ni-catalyzed aryl C(sp²)–H methylation (Scheme 1B).²⁵ Later,

several Ni-catalyzed alkylations of C(sp²)–H and N–H bonds with organic peroxides as the alkyl source were discovered (Scheme 1B).^{26–29} However, there is only one known example of Ni-catalysts that allows methylation at C(sp³)–H groups with dialkyl peroxides but with the additional assistance of Ir photoredox catalysis (Scheme 1C).³⁰

Importantly, although these transformations start by generating O-centered radicals, such species undergo fast fragmentation with the formation of alkyl radicals. Not only do these fragmentations waste the potential for forming a C–O bond but they are also undesirable for the activation of electron-rich C(sp³)–H bonds where electrophilic O-centered radicals would be preferred over C-centered radicals.³¹

Considering all of the above, one can ask what type of Ni-catalyst/peroxide system would enable oxidative C(sp³)–H functionalization? The present study answers this question, expands the catalytic potential of nickel in oxidative C–H functionalization with peroxides, and discloses a new reactivity pattern, i.e., oxidative ester formation (Scheme 1D).

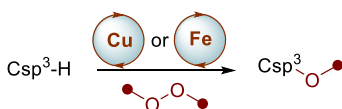
A suitable partner for such reactions could be diacyl peroxides, a readily available class of molecules used as radical initiators,³² oxidants, and sources of O- and C-functional

Special Issue: Organometallic Chemistry Inspired by Irina Beletskaya

Received: December 29, 2022

Scheme 1. Background of Metal/Peroxide Systems for Oxidative Functionalization

a) Kharasch-Sosnovsky reaction



b) Csp²-H alkylation with Ni/peroxide system

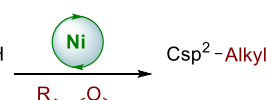
Chatani, 2016

Liu, 2017

Cal, 2017

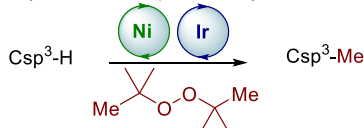
Guo, 2020

Maruoka, 2021



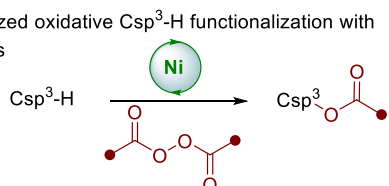
c) Csp³-H methylation with Ni/peroxide system

Stahl, 2021



d) This work:

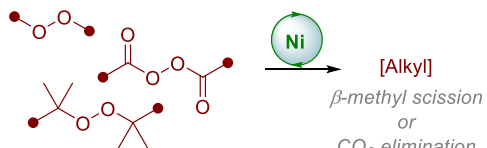
Ni-catalyzed oxidative Csp³-H functionalization with peroxides



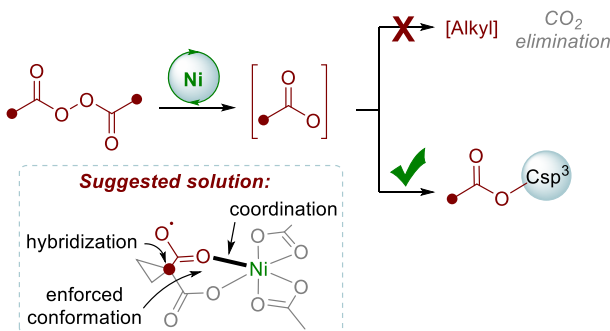
groups.^{33–35} Recently, cyclic diacyl peroxides^{36–41} have emerged as O-electrophilic reagents for the introduction of oxygen functionalities into alkenes,^{42–44} arenes,^{45–48} heterocycles,⁴⁹ and dicarbonyl compounds.⁵⁰ However, despite this popularity, organic peroxides have not been documented as acyloxylation agents in Ni-catalyzed processes (Scheme 2A).^{12,25–30,51} The main problem is that in Ni-catalyzed processes, the initially formed O-centered acyloxy radicals undergo fast elimination of CO₂, leading to C-centered radicals.^{12,51,52} Since CO₂ formation is fast,⁵³ selective processes involving the acyloxy radical are challenging.

Scheme 2. Use of Peroxides As Alkylation and Acyloxylation Reagents

a) Organic peroxides as an alkyl moiety source



b) This work: Organic peroxides as an acyloxy moiety source



Hence, the key question that we had to address is how to prevent decarboxylation of carboxy radicals. Only once this problem is solved, one can redirect these species for productive oxidative C–H functionalization.

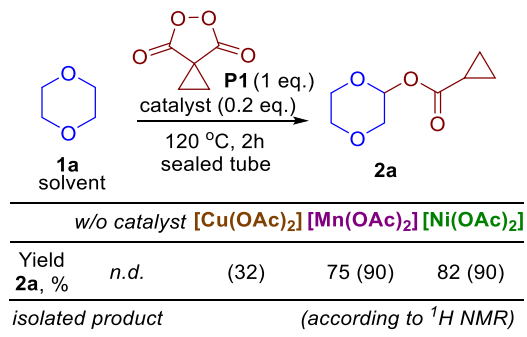
Recently, we communicated how to create metal-bound carboxylate radicals via the reaction of diacyl peroxides with Ni(OAc)₂.⁵⁴ An interesting mechanistic feature of the Ni insertion in the O–O bond is the transformation of a soft unreactive metal-centered radical at Ni(II) into a highly electrophilic O-centered carboxy radical that is capable of efficient C–H activation but also relatively stable toward the loss of CO₂. We have also identified structural features that allowed us to leverage this process for Ni-catalyzed C(sp³)-H acyloxylation of ethers (Scheme 2B). This reaction took dual advantage of diacyl peroxides as both an oxidant capable of generating high-valent Ni species and as a source of an acyloxy fragment.

Herein, we explore the organic chemistry aspects of this potentially rich chemistry including structural effects that prevent decarboxylation, a previously undisclosed stereo-electronic effect at the intersection of organic and coordination chemistry, as well as analysis of activating and deactivating stereoelectronic factors in the C–H activation step. We also show that the combination of stabilized carboxylate radicals with an unusual Ni(II)/Ni(III) catalytic cycle expands the scope of the new Csp³-H acyloxylation to ketones and alkanes (Scheme 1D and Scheme 2B).

RESULTS AND DISCUSSION

The initial focus was on the most active catalyst, [Ni(OAc)₂] in the model reaction of 1,4-dioxane (1a) with cyclopropyl malonoyl peroxide (P1) (Scheme 3). In a number of studies α -

Scheme 3. [Ni(OAc)₂] as a Leading Catalyst of Dioxane Acyloxylation



acyloxy-ethers were synthesized with peroxides by using Cu or Fe-catalysis.^{17,55–67} There is no reaction between 1,4-dioxane and peroxide P1 without a catalyst (Scheme 3). The reactions with [Cu(OAc)₂] and [Mn(OAc)₂] led to acyloxyated ether 2a in 32% and 75% yields, respectively. The highest yield of 2a was achieved using [Ni(OAc)₂] (82% isolated yield).

The other Ni salts provided lower yields of 2a (Table S1), so the carboxylate moiety is also important. The structures of the obtained [Ni(OAc)₂] catalyst was analyzed by scanning electron microscopy (SEM) and energy-dispersive X-ray spectroscopy (EDX) (see the Supporting Information). A hot filtration test demonstrated that the catalytically active species are transported from the solid into the solution (see the Supporting Information).

On the Formation and Electronic Structure of Ni (III) Species.

An interesting feature of this system is the oxidative addition of the peroxide to the metal.⁵⁴ Computational analysis suggests that the catalyst exists in several forms (“a cocktail of catalysts”),^{68,69} which result from the exchange of coordinating ligands and a variety of bonding modes and spin states. Here and below, more information on the results of the calculations and more details on some of the figures and schemes are included in the *Supporting Information*. In its monomeric form, Ni(II)-acetate is a triplet diradical. The most favorable oxidative addition of the metal catalyst to the peroxide occurs in the triplet state leading to one of two interconverting Ni-species, intermediates **C** and **D** (Figure 1A). Similar

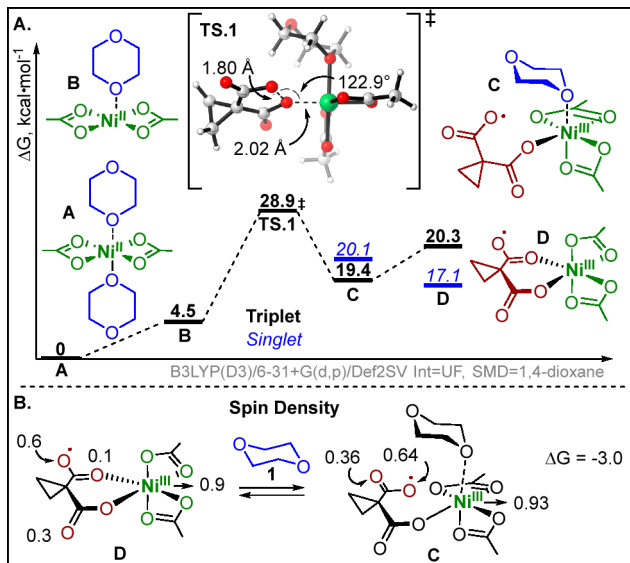
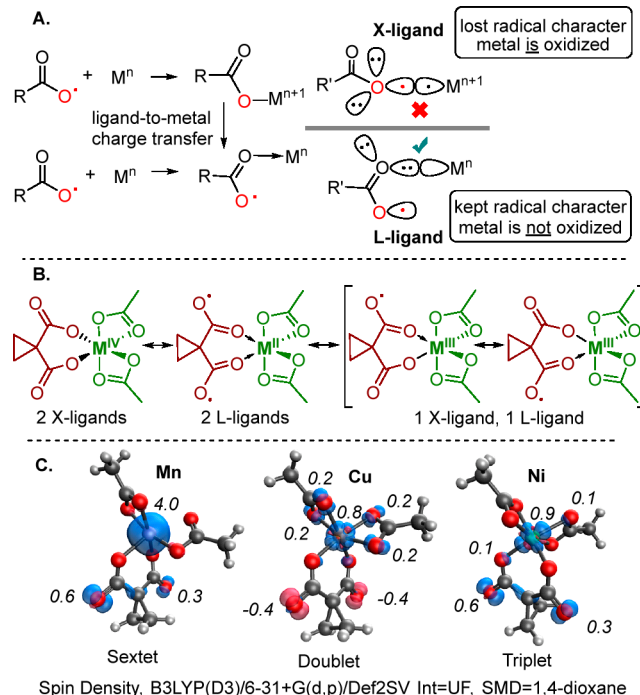


Figure 1. (A) Oxidative addition pathway resulting in the formation of the key Ni-intermediates. (B) Spin density of the two key Ni-intermediates **C** and **D**.

interconversion was observed for Fe(V)/Fe(IV) catalytic species with carboxylate ligands.⁷⁰ The spin density of both of these triplet diradicals clearly identifies a radical carboxylate moiety (Figure 1B). The Ni-assisted O–O bond activation transition state is readily accessible at the reaction conditions as it is ~ 29 kcal/mol above the most stable of the Ni-species in the catalytic cocktail.

A fascinating conclusion is that carboxylate can act as a noninnocent ligand in intermediate **D** that, like a chameleon, adopts several patterns when bonding to redox-active transition metals (Scheme 4A). If both carboxyl radicals, formed from O–O scission of the malonoyl peroxide, were to act as one-electron X-ligands toward Ni(II), the metal would have a formal +4 charge and the intermediate would have no radical character (Scheme 4B). On the other hand, if both carboxyl radicals were to act as two-electron L-ligands through the lone pairs on oxygen, the metal will not be oxidized further and the peroxide ligand will maintain its diradical character. Alternatively, a combination of the two ligand types could occur, where one carboxyl radical would act as an X-ligand and the other would act as a L-ligand. The combination of an X- and a L-ligand would result in an oxidized +3 metal, and significant radical character would remain on the peroxide ligand.

Scheme 4. (A) Two Ways to Use Carboxylate As a Ligand for the Formation of M–O Bonds, (B) Potential Oxidation States of the Intermediate Derived from $M(OAc)_2$ after Oxidative Insertion into the Peroxide, and (C) Spin Density (In Selected Spin States) Of the Catalytic Metal Complexes Accessible at the Reaction Conditions Shows the Carboxyl Radical Behaving as a L-Ligand⁵⁴



⁵⁴Figure adapted from ref 54. Copyright 2022 American Chemical Society.

How would a metal “decide” between L- over X-ligand behavior? When a radical behaves as an X-ligand, the metal provides one electron for the M–O bond and, hence, is formally oxidized (Scheme 4A). On the other hand, if a metal is reluctant to be oxidized further than the payoff of forming a covalent M–O bond may not be enough to compensate for the cost of going from M^n to M^{n+1} . Instead, an empty orbital of the metal may form a dative M–O bond with a lone pair of the oxygen (an L-ligand). Hence, whether the carboxyl radical will serve as an X- or L-ligand depends on the redox potential of the metal. Our analysis of the X/L ligand dichotomy identified several catalytically relevant transition metal complexes that retain significant radical character at the carboxylate ligands (Scheme 4C).

We suggest that the metal catalyst plays two major roles in the reaction: (1) assisting in O–O bond opening in the malonoyl peroxide through attack of the metal at one of the peroxide oxygens and (2) capturing the carboxyl radicals formed as a result of the O–O scission (Scheme 4A). These two roles define conflicting requirements from the metal. The metal needs to be electron rich in order to assist in opening the peroxide O–O bond but it also has to be able to resist oxidation by the carboxyl radical (i.e., carboxyl radical needs to serve as an L-ligand rather than an X-ligand). In our previous work, it was determined that Ni is the best choice out of the first-row transition metals for balancing the two requirements. The key mechanistic details of the activation step were disclosed in our recent communication⁵⁴ and will not be

repeated here. Instead, we will concentrate on electronic and stereoelectronic effects that control stability, reactivity, and selectivity of the metal-coordinated carboxyl radicals.

Importance of the Cyclopropyl Linker. An unusual feature of the C–H activation cascade reported herein is that the RCO_2 radical species do not undergo decarboxylation with the formation of a less reactive radical R but instead participate in H-abstraction from a suitable C–H bond. Considering that the decarboxylation process is known to be general,⁵³ direct C–H activation by the O-centered radical can only be efficient if H-abstraction is faster than decarboxylation.

Figure 2A illustrates that cyclopropyl malonoyl peroxide is the only cycloalkyl malonoyl peroxide that can efficiently

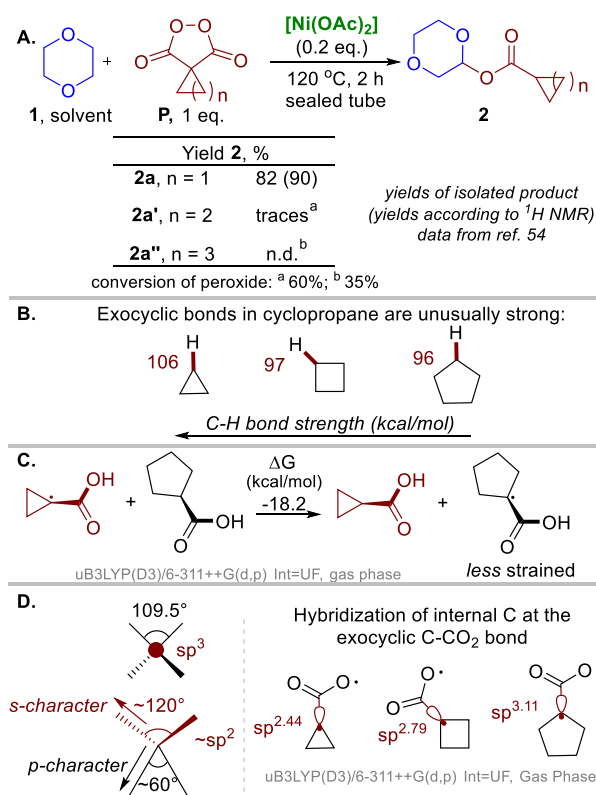


Figure 2. (A) Experimental yields for various sizes of cyclic linkers on the malonoyl peroxide. (B) Exocyclic C–H bonds on cyclopropane have a much higher BDE than for other cycles. Values are from ref 73. (C) Forming a radical on the cyclopropyl carbon is 18 kcal/mol higher in energy than forming a radical on the cyclopentane carbon. (D) Unusual properties of the exocyclic cyclopropane bonds originate from the hybridization required to form the small cycle.

acyloxylate dioxane.⁵⁴ A mixture of di- and monocarboxylic acids was also observed in the reaction mixtures in the case of cyclobutyl- and cyclopentyl malonoyl peroxides. We suggest that this is a consequence of different decarboxylation rates that originate from the differences in the stability of the forming carbon-centered radicals (Figure 2B–D). Indeed, the thermodynamic comparison in Figure 2C reveals that the cyclopropyl radical is destabilized by 18 kcal/mol relative to the cyclopentane radical.

The difference between cyclopropane and the larger cycles stems from frustrated hybridization (Figure 2D). It is well-known that exocyclic C–R bonds in cyclopropanes have greatly increased s-character. For example, the C–H bonds are approximately sp^2 -hybridized and, hence, are ~ 10 kcal/mol

stronger than the $\sim \text{sp}^3$ -hybridized C–H bonds of cyclopentane.⁷¹ Apparently, the effect is even larger for the C– CO_2 bond scission in 1,1-dicarboxy-substituted cycles (~ 18 kcal/mol, Figure 2C).

The origin of these effects is that the radical-bearing carbon atom in cyclopropane is unable to direct p-character toward the radical orbital because a large amount of p-character has already been used in making the endocyclic banana C–C bonds (Figure 2D). In the absence of structural or electronic constraints, breaking a covalent C–X bond at a “ sp^3 -carbon” converts this bond into a p-rich radical orbital. Because the total p-character at carbon is conserved, rehybridization at the radical center leads to rehybridization of the remaining C–R bonds at the radical carbon (i.e., $\sim \text{sp}^2$ hybridization for an acyclic radical). Such rehybridization increases the R–C–R angle in the radical relative to the tetravalent precursor⁷² and, hence, is difficult to attain in small strained cycles. In particular, the cyclopropyl carbon already directs increased p-character toward the endocyclic “banana” C–C bonds in order to narrow the C–C–C angles. If the p-character is redirected toward the radical center in the cyclopropyl radical, there is less p-character available for the ring bonds. Such suboptimal hybridization increases ring strain in the product.

As a result, the cyclopropyl linker partially protects the RCO_2 -radicals from undergoing decarboxylation. This effect is visible in the calculated thermodynamics of decarboxylation of malonoyl peroxides, both without the Ni-catalyst and coordinated at the Ni(III)-center for intermediates C and D (Figure 3). However, the story is more complex, in addition to hybridization of the cyclic linkers, another, previously unknown, layer of protection exists for the Ni-coordinated radicals. The barriers for decarboxylation from the malonoyl peroxide derivatives show the protecting effect of the cyclopropyl spiro-cycle (Figure 3A). The cyclopropyl linker has the highest barrier for decarboxylation, with a barrier 2.5–4.4 kcal/mol higher than for the other cycles. Interestingly, the relationship with the ring size is not simple as the cyclopentane group has a larger barrier for decarboxylation than the cyclobutane group (4.1 vs 2.2 kcal/mol, respectively). Intrigued by these observations, we analyzed the reactant and transition state geometries and found large differences in the orbital alignments.

An additional layer of stereoelectronic protection is found in the orbital alignments of the reactants and transition states. For both free carboxyl radical examples (i.e., the catalyst-free system and the Ni-bound monodentate intermediate C), the alignment of the carboxyl radical groups with the C–C bonds of the ring is noticeably different for the different ring sizes (Figure 3B). In particular, the two carboxyl groups connected by the cyclopropyl linker remained in the same plane, likely to maximize the donor–acceptor interactions between the banana bonds of the ring and the carbonyl group. On the other hand, the two carboxyl groups at the 4- and 5-membered cyclic linkers aligned perpendicularly to each other, with each carboxyl group in-plane with a different cyclic $\sigma_{\text{C–C}}$ bond.

In contrast, the simultaneous coordination of both carboxyl groups with the Ni(III) center in the bidentate intermediate D enforces the same conformation for the different ring sizes (Figure 3E). The enforced conformation is the same one as the preferred geometry for the cyclopropyl case but corresponds to a higher energy conformation for the cyclobutane and cyclopentane systems. The loss of σ -conjugation interactions for the cyclobutane and cyclopentane groups raises the energy

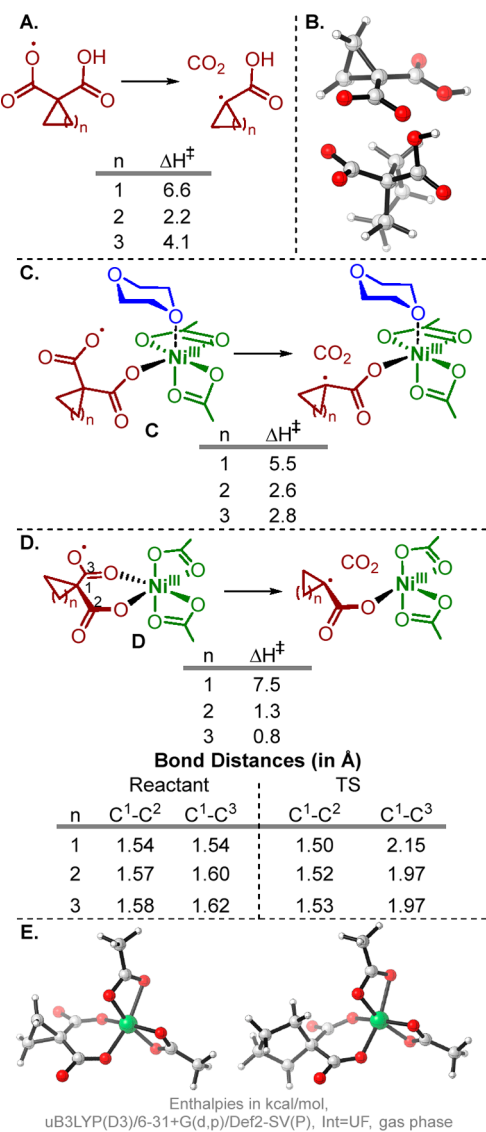
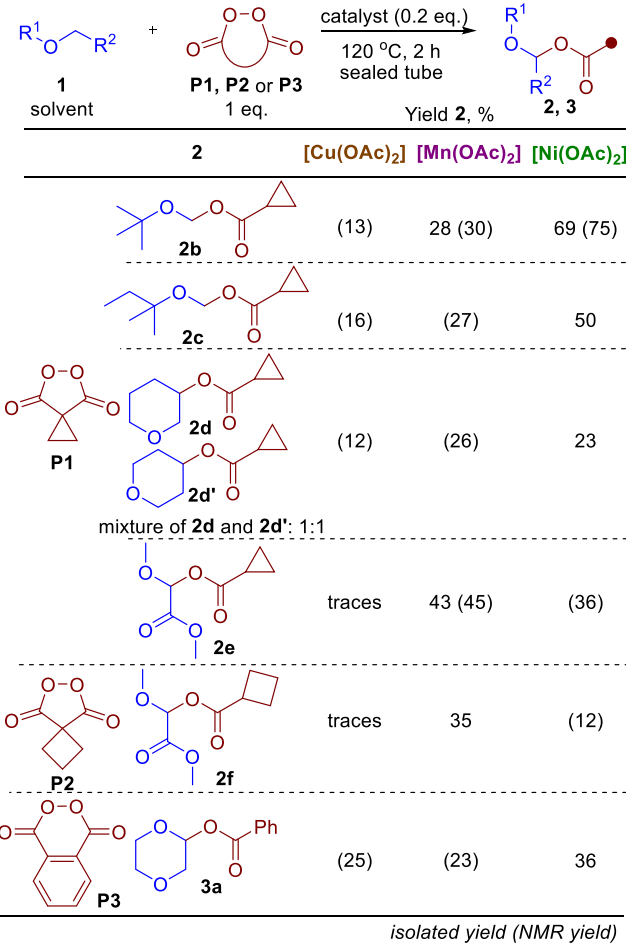


Figure 3. (A) Impact of hybridization on the activation barrier for decarboxylation without the Ni-catalyst. (B) Difference in carboxyl group orientation for cyclopropyl and cyclopentane carboxylates. (C) In intermediate C, the free carboxyl radical retains conformational mobility resulting in comparable barriers to decarboxylation as part A. (D) Carboxyl groups are forced into the same plane when coordinated to Ni(III) in intermediate D. The bond distances show that decarboxylation from the cyclopropyl group has a much later transition state than for the other cycles. (E) Carboxyl group orientation in intermediate D for cyclopropyl and cyclopentane systems.

of the reacting radicals and lowers the activation barriers for their decarboxylation while the barrier for the loss of CO₂ in the cyclopropyl system is slightly increased (Figure 3D). In summary, the same coordination effects that deactivate and “protect” the cyclopropyl system appear to have the opposite effect on the larger cycles, making the loss of CO₂ nearly barrierless for cyclobutane and cyclopentane spiro-cycles.

Scope of the Oxidative Acyloxylation. In an attempt to explore the scope of oxidative acyloxylation of ethers, we investigated the possibility of oxidation of various ethers with malonoyl peroxides (**P1** and **P2**) using the palette of catalysts, [Cu(OAc)₂], [Mn(OAc)₂], and [Ni(OAc)₂] (Scheme 5). Indeed, the Mn(OAc)₂ and Ni(OAc)₂ catalyzed reaction of

Scheme 5. Cu-, Mn-, or Ni-Catalyzed Oxidation of Ethers by Cyclic Diacyl Peroxides



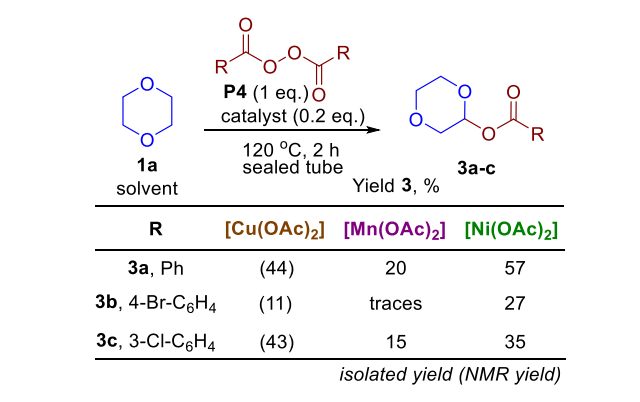
ethers **1b–e** with peroxide **P1** transformed them into acyloxy derivatives **2b–e** in 23–69% isolated yields (Scheme 5). There is a steady tendency of increasing the yield of the oxidative acyloxylation product when switching from the traditional copper catalysis to catalysis with manganese and nickel compounds. Cyclobutyl malonoyl peroxide **P2** and phthaloyl peroxide **P3** provided lower yields of acyloxylated products **2f** and **3a**. The main byproducts (Scheme 5) were cyclopropane-1,1-dicarboxylic acid, cyclobutanecarboxylic acid, and benzoic acid from peroxides **P1**, **P2**, and **P3**, respectively.

The regioselectivity of oxidative acyloxylation of ethers is noteworthy. Substrates **1b** and **1c**, which have primary and secondary C–H bonds, reacted only through the primary C–H bond at the α -position to the oxygen atom. This fact suggests that coordination assists the acyloxylation. On the other hand, tetrahydropyran **1d** formed acyloxylated products **2d** and **2d'** which correspond to the β -C–H bond and the γ -C–H bond activation. The potential stereoelectronic interactions contributing to the selectivity are discussed later.

Dibenzoyl peroxide **P4** reacted with 1,4-dioxane provided the product of oxidative acyloxylation **3a** in 20 and 57% yields in the case of [Mn(OAc)₂] and [Ni(OAc)₂] catalysts, respectively (Scheme 6).

Within the explored scope of diaryl peroxides **P4a–c**, the observed reactivity depended on the metal and the aryl group in a complex way. However, on average, one can conclude that the reactivity of [Cu(OAc)₂] in synthesis of **3a–c** was higher

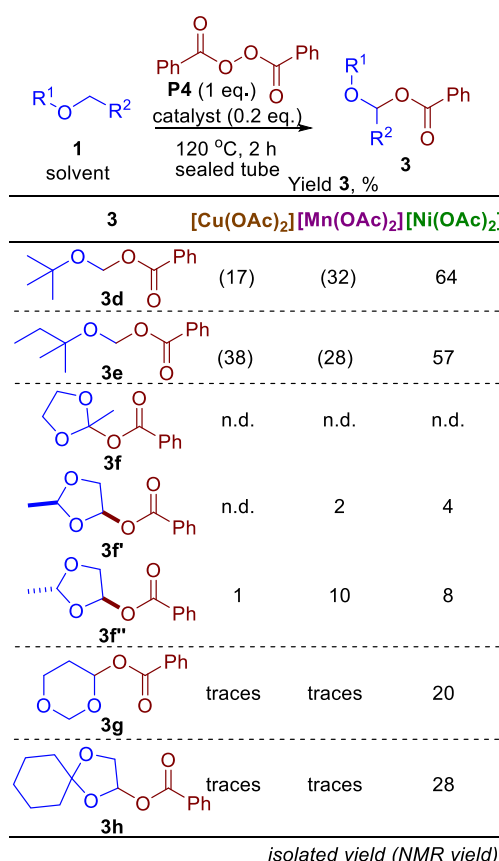
Scheme 6. Cu-, Mn-, or Ni-Catalyzed Oxidative Acyloxylation of 1,4-Dioxane by Non-Cyclic Diacyl Peroxides



than $[\text{Mn}(\text{OAc})_2]$ but still lower than $[\text{Ni}(\text{OAc})_2]$. The halo-substituents in the aryl ring of the peroxides lowered yields of acyloxylation products **3b** and **3c** compared to **3a**.

We also explored the catalytic activity of Cu-, Mn-, or Ni-catalysts in the reaction of dibenzoyl peroxide **P4** with a broad selection of ethers **1d–h** (Scheme 7). Products **3d–h** were obtained in 8–64% yields with the $[\text{Ni}(\text{OAc})_2]$ catalyst. It should be noted that application of $[\text{Cu}(\text{OAc})_2]$ led to lower **3d–h** yields. The regioselectivity patterns are similar to those with cyclic diacyl peroxides (Scheme 5). The main byproduct (Scheme 6 and 7) was benzoic acid.

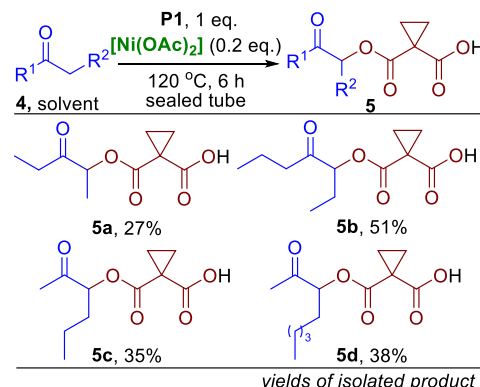
Scheme 7. Cu-, Mn-, or Ni-Catalyzed Oxidation of Ethers by Dibenzoyl Peroxide



Substrates **1b** and **1c** were acyloxylated only through the primary α -C–H bond with the formation of products **3d** and **3e**. For substrates that had α -C–H bonds surrounded by either one or two oxygen atoms, only the acyloxylation products through the former one (products **3f'**, **3f''**, and **3g**) were isolated, possibly due to the instability of the ortho ester fragment. The α -C–H bond near the acetal fragment did not contribute to the acyloxylation process, and the regio isomer **3h** was the only one isolated and detected by GC-MS analysis.

After successfully achieving good yields in $\text{C}(\text{sp}^3)$ -H acyloxylation of ethers with cyclic diacyl peroxides, we applied this protocol further for acyloxylation of ketones (Scheme 8).

Scheme 8. Ni-Catalyzed Acyloxylation of Ketones by Cyclopropyl Malonoyl Peroxide



In a few studies, α -acyloxylation of ketones were performed using Cu-catalysis,^{74–77} hypervalent iodine compounds,^{78–83} *N*-methyl-*O*-benzoylhydroxylamine hydrochloride,⁸⁴ or $[\text{Hal}]^-$ /electric current systems.^{85,86} Apart from these reports, α -acyloxy ketones were prepared by oxidative functionalization of enol derivatives.^{87,88}

We probed the reaction on simple ketones **4a–d**, the corresponding derivatives **5a–d** were obtained in 27–51% yields, demonstrating the generality of the carboxylate radical creation protocol. When there was a choice between primary and secondary C–H bonds in the α -position to the carbonyl group, only the secondary C–H bonds reacted (products **5c** and **5d**). Decarboxylation of the products was not observed; the main byproduct was cyclopropane-1,1-dicarboxylic acid.

Stereoelectronic Assistance in Ni(III)-Mediated C–H Activation. We have explored computationally the reaction of 1,4-dioxane with $[\text{Ni}(\text{OAc})_2]$, the most promising catalyst, in detail. Considering the products **2d** and **2d'** (Scheme 5), we investigated the possibility of β -hydrogen atom transfer (HAT) in 1,4-dioxane coordinated at the nickel. Remarkably, the calculated barrier of 8.5 kcal/mol would make the β -HAT nearly 10^5 times faster than α -HAT (Figure 4).

Hence, the anomeric stereoelectronic assistance is much more efficient in the absence of metal coordination at the adjacent oxygen. Such modulation of anomeric effect opens the possibility of remote activation. In the β -HAT process, both the 1,4-dioxane substrate and the bis-carboxy ligand at the catalyst serve as bifunctional reagents. Each of them uses one oxygen to coordinate at the metal, whereas the second ether oxygen (dioxane) or carboxy radical (malonate) are directly involved in a chemical transformation at a remote position. Such architecturally precise matching of the two functionalities suggests interesting design opportunities for future selective

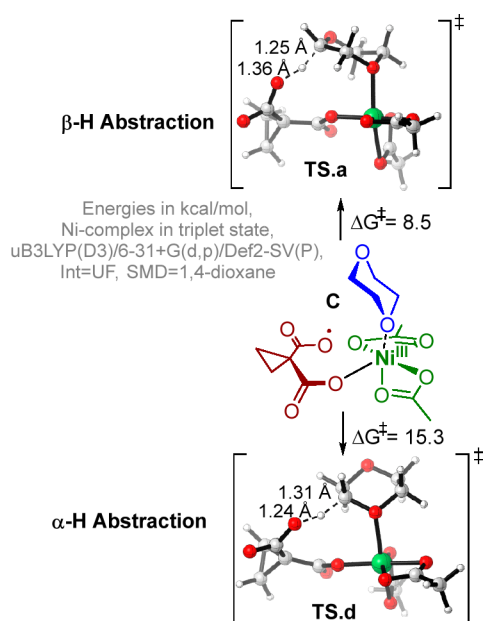


Figure 4. Reaction barriers for both α - and β -hydrogen abstraction using the malonyl peroxide ligand.

C–H activation reactions. Computations were performed in order to explore the impact of stereoelectronic assistance on the β -HAT barrier. In particular, we removed stereoelectronic assistance at the β -position by replacing the noncoordinating oxygen with carbon (i.e., using tetrahydropyran (THP) in place of 1,4-dioxane) (Figure 5). When stereoelectronic

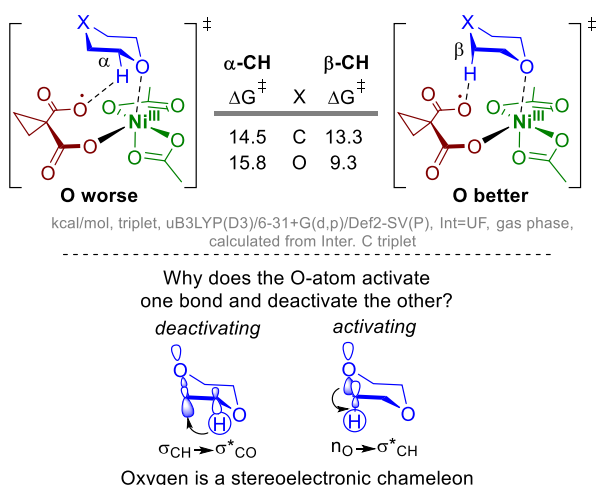


Figure 5. Investigating the role of stereoelectronic assistance in α - and β -HAT by removing the noncoordinating oxygen.

assistance is turned off, the barrier for β -HAT increases from 9.3 to 13.3 kcal/mol, indicating that the noncoordinating oxygen greatly contributes to the lower activation barrier at the β -position.

In addition, comparison of THP and 1,4-dioxane revealed an interesting remote stereoelectronic interaction between the β -oxygen and the α -C–H bond. In particular, the α -HAT in THP has a barrier of 14.5 kcal/mol, ~1.3 kcal/mol lower in comparison with the α -HAT in dioxane (15.8 kcal/mol).

These findings illustrate that the noncoordinating β -oxygen activates one C–H bond (the β -CH) but deactivates another

C–H bond (the α -CH). The ability to use the same structural element for two complementary purposes is perfect for achieving high selectivity, in agreement with the experimental data.

How can the same atom impose such contrasting effects at the adjacent C–H bonds? Oxygen is able to be both activating and deactivating because oxygen is a stereoelectronic chameleon capable of being either a strong donor or a strong acceptor, depending on its relative position to the affected C–H bond.^{89,90} For β -HAT in 1,4-dioxane coordinated with the metal at the α -oxygen (Figure 5, top), the noncoordinated β -oxygen acts as a strong donor via a $\sigma_{\text{O}} \rightarrow \sigma^*_{\text{CH}}$ interaction, assisting in breaking the C–H bond. However, for α -HAT, the β -oxygen acts as a strong acceptor via a $\sigma_{\text{CH}} \rightarrow \sigma^*_{\text{CO}}$ interaction that pulls electron density out of the α -CH bond making hydrogen less reactive toward the electron-deficient oxygen radical. Similar deactivating effects of the β -alkoxy substituent on C–H bonds were observed earlier in the Rh-catalyzed insertion into C–H bonds of ethers,⁹¹ a variety of transition metal-catalyzed C–H functionalizations of carbohydrates⁹² and radical C–H activation in diols.⁹³

The potential for the “closed” intermediate **D** to also perform HAT was explored due to the significant radical character on the carboxyl ligand in the intermediate (Figure 6). Unlike the “open” intermediate **C** where the HAT donor is bound to the HAT acceptor through the simultaneous metal coordination, in **D** the two species are not forced into close proximity by coordination to the metal. Despite dioxane not being directly bound to the metal-carboxyl intermediate, calculations located an enthalpically favorable complex which brings dioxane into close proximity of the carboxyl-ligand radical (Figure 6). The entropic penalty for bringing two molecules together takes most of the enthalpic stabilization away, so the overall free energy for the complex formation is close to zero. Nevertheless, the complex of intermediate **D** and dioxane is clearly accessible under the reaction conditions. The HAT from the complex is predicted to be very fast, the activation barrier is only 1 kcal/mol (1.5 kcal/mol relative to the two uncomplexed species). Interestingly, all attempts to locate a transition state for the complex of intermediate **D** with 1,4-dioxane in the boat conformer prior to HAT optimized directly to the H-abstraction product, **E** (Figure 6). The absence of a barrier can be attributed to several factors. Not only is the O-radical very electrophilic due to its close proximity to a Lewis acid but the target $\sigma_{\text{C–H}}$ bond is electron-rich due to the anisotropic $\sigma_{\text{O}} \rightarrow \sigma^*_{\text{C–H}}$ donation. Literature precedents suggest the boat conformer of 1,4-dioxane will be a favorable reaction partner due to the better array of stereoelectronic interactions involved in the “radical homoanomeric effect”.^{94,95} The calculations agree with the literature precedents, where once the boat is formed from the chair conformer (a process that costs 6.4 kcal/mol) the HAT from the boat is barrierless. The spin density evolution in the reaction is consistent with radical H-transfer. In reactant **D**, the noncoordinated oxygen has substantial spin density, while in **E** there is no spin density on the oxygen after the O–H bond is formed, suggesting a HAT mechanism (Figure 6).

Mechanism. On the basis of the computational and experimental results, we propose that the reaction starts with metal-mediated O–O ring opening of malonyl peroxide **P1** with Ni(II) acetate to give the Ni-bound monodentate intermediate **C** (Scheme 9). This intermediate can interconvert with a nearly isoenergetic Ni-complex **D**.

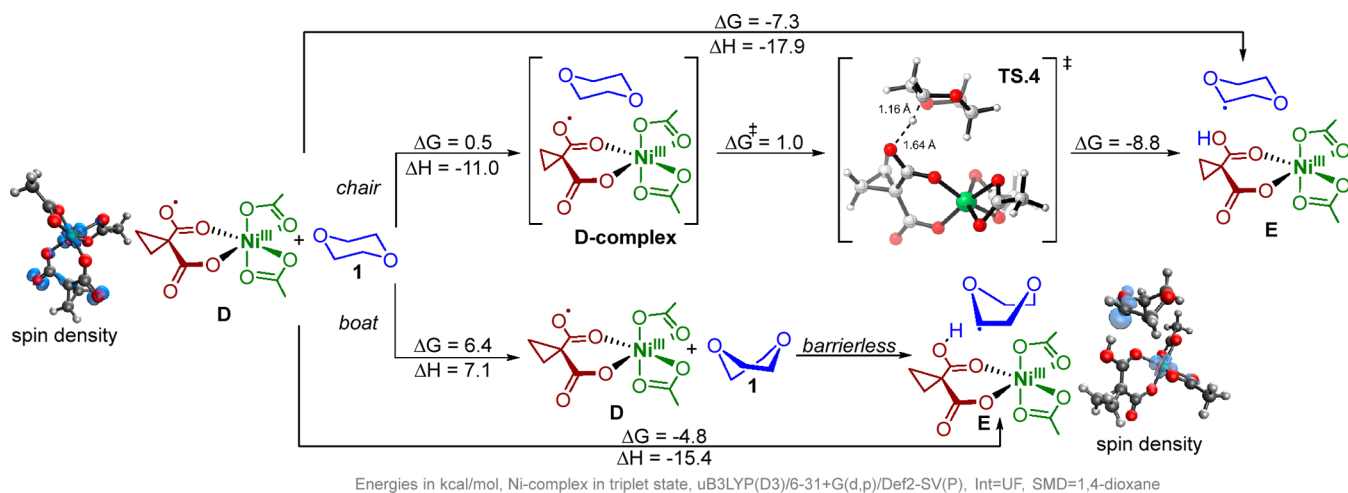
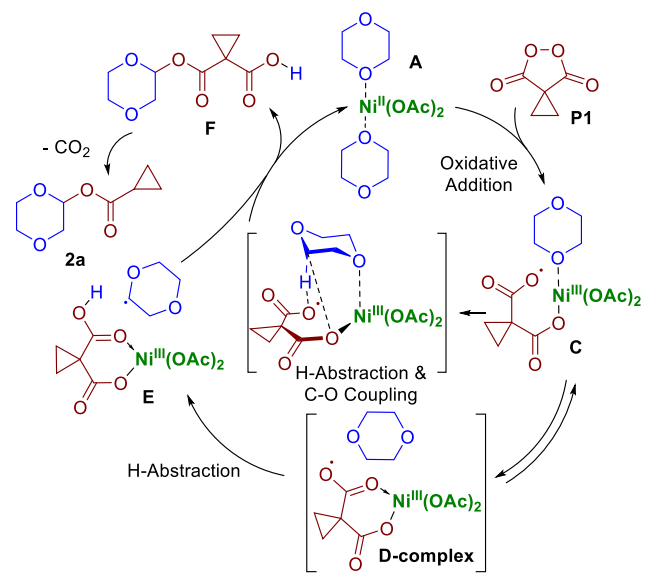


Figure 6. HAT from noncoordinated 1,4-dioxane in both the chair and boat conformer using the carboxyl radical of intermediate D.

Scheme 9. Proposed Mechanism for the Oxidative Acyloxylation of Ethers Using Two Ni(III)-Complexes



Both Ni-intermediates maintain radical character on the peroxide ligand, therefore either one of these two reactive Ni-species can activate the C–H bond in 1,4-dioxane. HAT from the coordinated and non-coordinated dioxane molecule is assisted by stereoelectronic interactions (anomeric effect, deactivated anomeric effect, and radical anomeric effect). H-abstraction from intermediate C appears to be followed by barrierless C–O coupling, potentially facilitated by the metal-center. On the other hand, a stepwise process is likely to occur for the L-ligand Ni-species, intermediate D-complex. H-abstraction from dioxane forms the carbon radical, intermediate E. At this point the two mechanistic pathways converge, giving intermediate F and regenerating the starting catalyst A. Decarboxylation of F affords product 2a.

C–H Activation in Alkanes. The above prediction of fast HAT from dioxane to the Ni(III) intermediate D is intriguing because it suggests that the C–H containing molecule does not need to be coordinated to the metal for HAT to occur. Our calculations with dioxane suggest that the Ni(III) species retains enough radical character to be sufficiently reactive, perhaps even toward unactivated substrates (Figure 6).

Motivated by these findings, we decided to explore if the catalytic system can activate alkanes, the ultimate target of C–H activation. The direct C–H functionalization of non-activated alkanes is still relatively scarce due to their intrinsic low reactivity. Acyloxylation of C(sp³)–H bonds in alkanes was achieved with [Au]/PIDA,⁹⁶ Co(OAc)₂/I₂/NHPI/O₂/HNO₃,⁹⁷ H₂O₂/TFA,⁹⁸ Selectfluor/CuBr₂/pentanenitrile,⁹⁹ TFAN/TFA,¹⁰⁰ RuCl₃/AcOOH/TFA,¹⁰¹ Fe(III)/O₂/TFA/*h*v,¹⁰² and [Mn]/H₂O₂.^{103,104} In some cases, it was difficult to avoid overoxidation of the product, which led to allyl esters (CuTPP/DTBP,¹⁰⁵ Cu(OAc)₂/TBHP,¹⁰⁶ [(BPI)CuCl]/DTBP,¹⁰⁷ and CuO/DTBP¹⁰⁸).

The possibility of acyloxylation of nonactivated Csp³-H bonds was investigated using a selection of alkanes. Cyclohexane reacted with cyclic diacyl peroxides P1 and P3 to afford the corresponding products 7a and 7b in good yields using the Ni(OAc)₂-catalyst (Scheme 10). Dibenzoyl peroxide P4 gave product 7b in low yields.

Scheme 10. Cu-, Mn-, or Ni-Catalyzed Oxidation of Cyclohexane by Diacyl Peroxides

6a solvent	P 1 eq.	catalyst (0.2 eq.)	120 °C, 8 h sealed tube	Yield 7, %
Peroxide	Product	[Cu(OAc) ₂]	[Mn(OAc) ₂]	[Ni(OAc) ₂]
P1	7a	(48)	(51)	75 (80) 72*
phthaloyl peroxide P3	7b	(34)	(35)	48
P4	7b	n.d.	traces*	10*

* EtOAc cosolvent isolated yield (¹H NMR yield)

We have also evaluated energy profiles for the key H-atom abstraction computationally. The activation barrier for HAT from cyclohexane is approximately 7 kcal/mol larger than for 1,4-dioxane (Figure 7). The low barrier for HAT from 1,4-dioxane is not surprising due to the stereoelectronic assistance activating the C–H bond in this O-containing molecule.

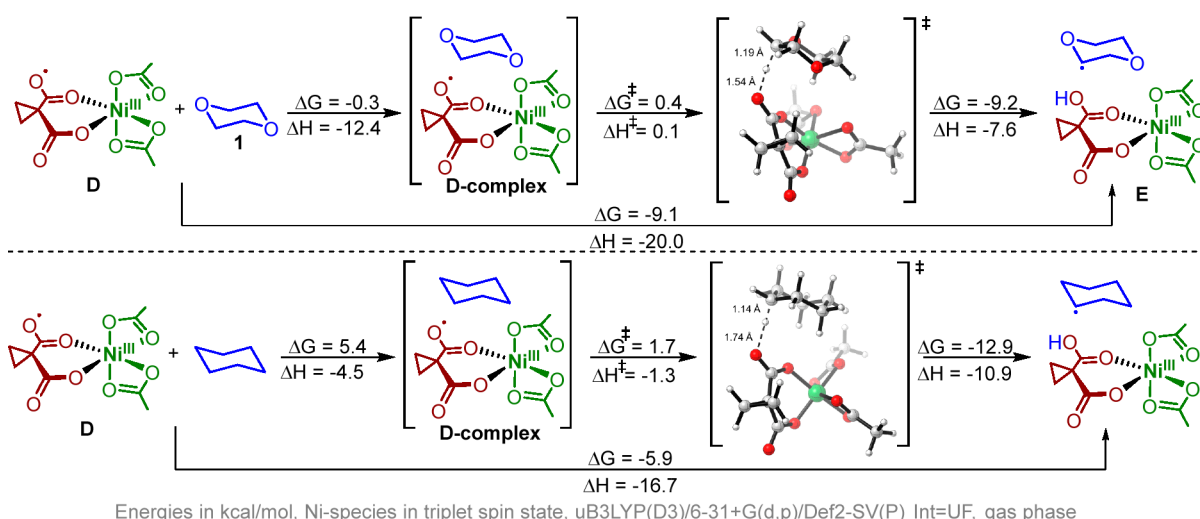


Figure 7. Comparison of the barriers of H-abstraction from 1,4-dioxane vs cyclohexane. The TS is nearly energy neutral for 1,4-dioxane starting from the separate reactants. The activation barrier for cyclohexane is approximately 7 kcal/mol.

Cyclohexane has no intramolecular stereoelectronic assistance to lower the activation barrier.

A selection of alkane substrates were examined to evaluate this process (Scheme 11). First, cycloalkanes were explored with malonoyl peroxide **P1**, phthaloyl peroxide **P3**, and dibenzoyl peroxide **P4**. Generally, cyclopropyl malonoyl peroxide **P1** worked the best to give the esters **8a**, **8c**, and **8e** in 57–76% yield. The yields of the products with phthaloyl peroxide **P3** and dibenzoyl peroxide **P4** (**8b**, **8d**, **8f**) were lower. Several other alkanes like 2,3-dimethylbutane, methylcyclopentane, 3-methylpentane, and *n*-hexane gave the desired products **8g–k** in moderate to good yields. However, for the last three substrates, the reaction produced a relatively complex mixture of regiosomers with only slight preference for the functionalization product of the most substituted carbon atom. The low regioselectivity is consistent with the very low calculated barrier for the C–H abstraction step. Comparing the reactivity of C–H bonds in substrates **6i–k**, it becomes clear that the tertiary C–H bonds are 60–90 times more reactive than primary C–H bonds. The reactivity of the secondary C–H bonds is 8–23 times higher than that of the 1° C–H bonds. It is necessary to use a cosolvent to achieve good yields probably because of the insolubility of peroxides in alkanes. Interestingly, EtOAc was inert under the reaction conditions and can serve as a suitable reaction media. It should be noted that no other alkane oxidation products were observed (Scheme 11).

We also tested if our Ni-catalyzed acyloxylation strategy can be extended to various aromatic compounds with benzylic C(sp³)–H bonds (Scheme S2). For these cases, complex mixtures of oxidation products were formed, according to GC–MS. Unfortunately, selective C(sp³)–H acyloxylation was not observed.

In order to better understand the importance of coordination between the active catalyst and substrate (intermediate **C** vs **D** in the computational pathway), we carried out the reaction with an equimolar mixture of 1,4-dioxane and cyclohexane (Scheme 12). Surprisingly, the yield of the dioxane- and cyclohexane-derived products **2a** (29%) and **7a** (34%) were comparable, which means the coordination is not obligatory for the target acyloxylation. Taking into account the number of C–H bonds in 1,4-dioxane (8) and cyclohexane

(12), one can conclude that the C–H bond in 1,4-dioxane is only ≈1.3 times more reactive than the C–H bond in cyclohexane.

In order to investigate the nature of the rate-determining step (RDS), we carried out kinetic isotope studies with deuterated cyclohexane (Scheme 13). The deuterium isotope effect of 7.3 was observed, which leaves two possibilities: either (1) C–H activation is the RDS or (2) C–H activation (i.e., the “Product-Determining Step”) occurs after the RDS.¹⁰⁹ Computational results (Figure 8) suggest that peroxide activation by the catalyst (which must occur before C–H activation) is the RDS, in general agreement with the experimental results. So where is the rate-determining step? The experimental results suggest that is either before C–H activation or C–H activation itself while computational results suggest that it is peroxide activation by the catalyst.

CONCLUSION

Reaction with cyclic diacyl peroxides can transform a soft unreactive metal-centered radical at Ni(II) into a highly electrophilic metal-bound O-centered carboxy radical that is capable of efficient C–H activation. We show that such radicals can be used for nickel-catalyzed C(sp³)–H oxidative functionalization as long as their decarboxylation is prevented by combining two levels of protection, i.e., hybridization and stereoelectronics.

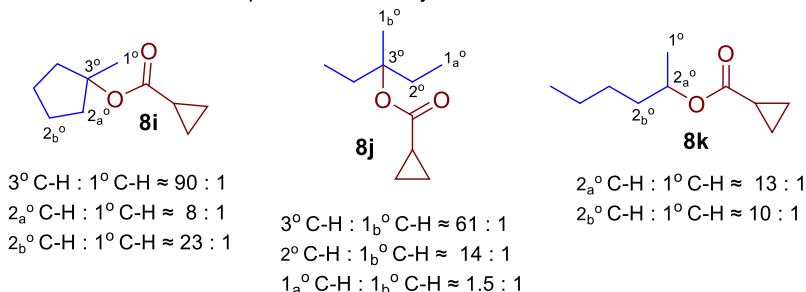
In particular, the cyclopropyl linker plays a special role in stabilization of carboxylate radicals because it provides dual stereoelectric protection from decarboxylation on the order of 6–7 kcal/mol relative to the larger rings. At the first “hybridization” level of protection, as the cyclopropyl carbon directs increased p-character toward the endocyclic “banana” C–C bonds, the C–CO₂ bond-forming hybrid has greater s-character, with concomitant bond shortening and strengthening, in comparison to the other systems. At the second “stereoelectronic” level, the enforced planar conformation of both carboxyl groups with the Ni(III) center in the bidentate intermediate **D** is the same one as the intrinsic preferred geometry for the cyclopropyl case but corresponds to a higher energy conformation for the cyclobutane and cyclopentane systems. This is a new stereoelectronic effect originating from a combination of organic and coordination chemistry.

Scheme 11. Ni-Catalyzed Oxidation of Alkanes by Diacyl Peroxides

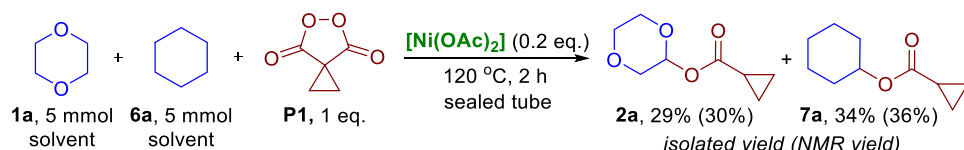
6, solvent	1 eq.	[Ni(OAc) ₂] (0.2 eq.)	120 °C, 8 h	EtOAc	8
Peroxide	Product 8	Yield 8, %	Peroxide	Product 8	Yield 8, %
P1		18*	P1		21*
P3		47	P3		52
P4		traces	P4		40
P1		73	P1		61
P3		50	P1		40
P4		20			
P1		76	P1		62
P3		53	P4		26
P4					

yields of isolated product (yields according to ¹H NMR) * rxn without EtOAc

Comparative reactivity of each C-H bond



Scheme 12. Ether/Alkane Competition in Ni-Catalyzed Acyloxylation by Cyclopropyl Malonoyl Peroxide



In addition, coordination to the metal center provides a supplementary way to control stability and reactivity of carboxylate radicals. The transition metals can interact with the RCO₂-moiety in two ways, i.e., by accepting either one or two electrons from the oxygen for M–O bond formation. In other words, in the presence of the right metal partner, the carboxylate ligand becomes “non-innocent”. In the high-valent radical Ni-species, produced in the reaction of Ni(II) and

diacyl peroxides, one or both carboxylate fragments derived from diacyl peroxide can serve as an X-ligand which retains significant radical character on the carboxylate oxygens (Figure 8). It is the presence of spin density on the carboxylate fragment (the O-radical) that allows the following C–H activation via radical H-atom transfer from the substrate. Computations proved that the HAT step can be realized both from the “open” intermediate C where the HAT donor is

Scheme 13. (Top) Kinetic Isotope Effect Experiment and (Bottom) (A) No D-Effect on Rate and Product Ratio; (B) Primary D-Effect on Rate and Product Ratio; and (C) No Effect on Rate, Primary D-Effect on Ratio

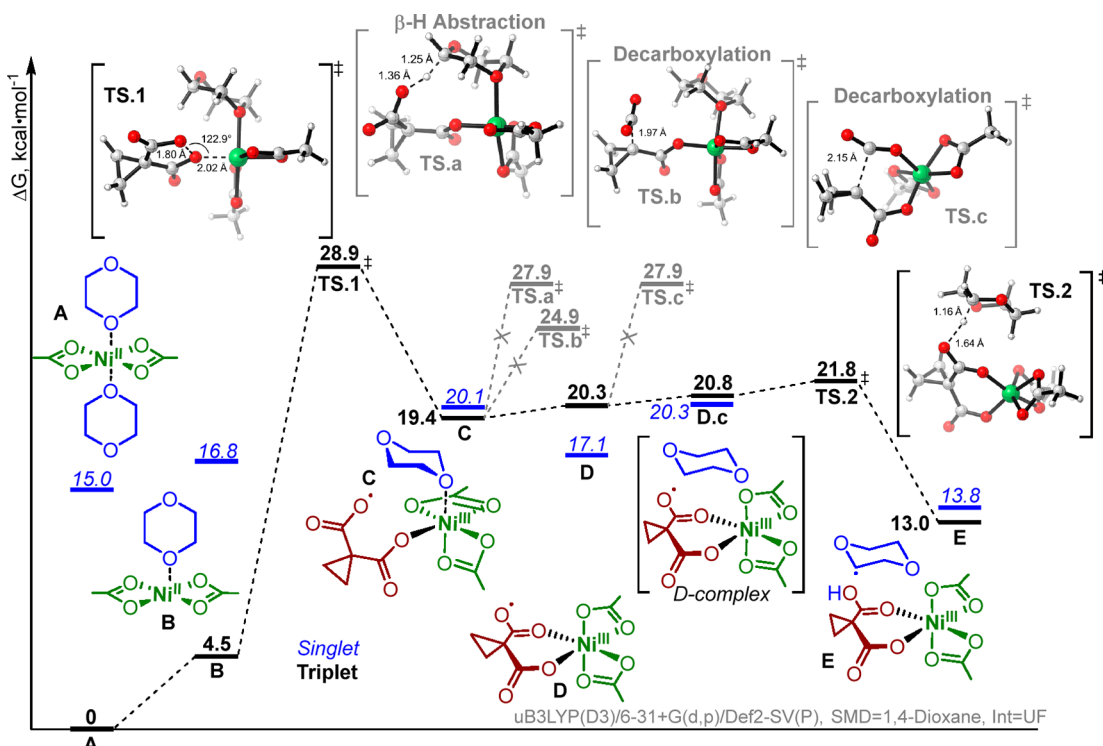
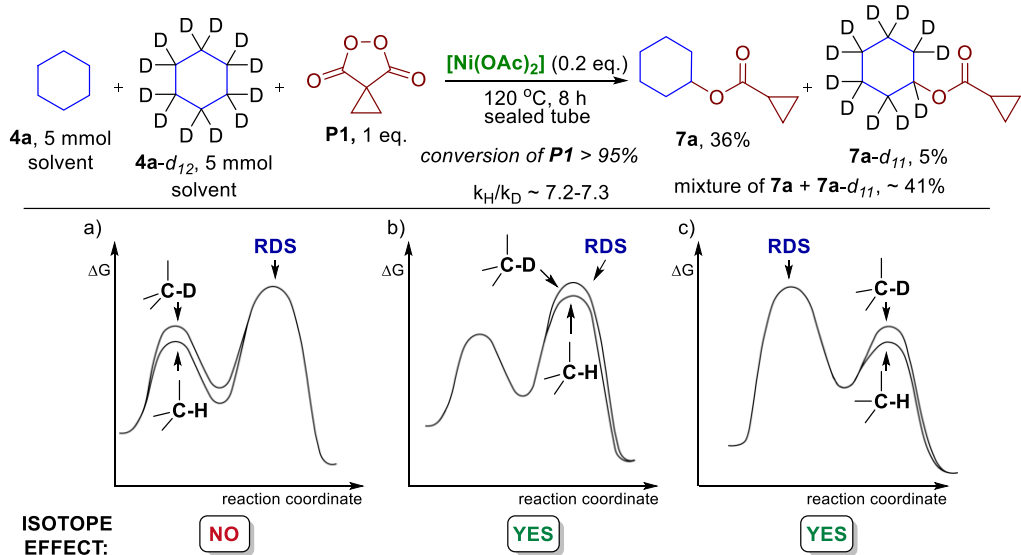


Figure 8. Total potential energy surface for the oxidative acyloxylation of 1,4-dioxane using a Ni(III)-complex.

bound to the HAT acceptor through the simultaneous metal coordination and from “closed” intermediate D (D-complex) where the two species are not forced into close proximity. This finding explains the observed alkane functionalization as well as the selectivity of ether and ketone acyloxylation.

The main mechanistic features of the new transformation are (1) the rate-determining oxidative addition of the O–O bond to the nickel center, resulting in a dynamically interconverting mixture of catalytic Ni-species in the formal Ni(III) state (intermediate **C** and **D**-complex) and (2) the possibility of HAT with or without substrate coordination to the metal center.

The scope of the new oxidative acyloxylation with diacyl peroxides spans activated electron-rich (ethers), activated electron-deficient (ketones), and nonactivated substrates (alkanes). These reactions open a direct synthetic connection between hydrocarbons and esters. The selectivity of the oxidation among various C–H substrates was higher with nickel acetate than with copper and manganese salts, the traditional catalysts for the Kharasch reaction.

The ability of diacyl peroxides to unlock high valent Ni chemistry is another illustration of the underutilized potential of this still often misunderstood organic functionality^{110,111} for the design of new reactions. Combining organic peroxides with

transition metal catalysis should provide new contributions to the renaissance of organic peroxide chemistry.^{112–115}

■ ASSOCIATED CONTENT

SI Supporting Information

The Supporting Information is available free of charge at <https://pubs.acs.org/doi/10.1021/acs.organomet.2c00663>.

Stationary points for C–H substrates, diacyl peroxides, and Ni-complexes (XYZ)

Experimental procedures, characterization data of catalyst and synthesized compounds, and computational calculations (PDF)

■ AUTHOR INFORMATION

Corresponding Authors

Alexander O. Terent'ev – *N. D. Zelinsky Institute of Organic Chemistry, Russian Academy of Sciences, Moscow 119991, Russian Federation*;  orcid.org/0000-0001-8018-031X; Email: terentev@ioc.ac.ru

Igor V. Alabugin – *Department of Chemistry and Biochemistry, Florida State University, Tallahassee, FL 32306, United States*;  orcid.org/0000-0001-9289-3819; Email: alabugin@chem.fsu.edu

Authors

Vera A. Vil' – *N. D. Zelinsky Institute of Organic Chemistry, Russian Academy of Sciences, Moscow 119991, Russian Federation*;  orcid.org/0000-0002-6847-6035

Yana A. Barsegyan – *N. D. Zelinsky Institute of Organic Chemistry, Russian Academy of Sciences, Moscow 119991, Russian Federation*

Leah Kuhn – *Department of Chemistry and Biochemistry, Florida State University, Tallahassee, FL 32306, United States*

Complete contact information is available at:

<https://pubs.acs.org/10.1021/acs.organomet.2c00663>

Author Contributions

The manuscript was written through contributions of all authors. All authors have given approval to the final version of the manuscript.

Notes

The authors declare no competing financial interest.

■ ACKNOWLEDGMENTS

The synthesis of peroxides and the oxidative C–H functionalization experiments were supported by the Russian Science Foundation (Project 21-73-10016). I.A. is grateful to the National Science Foundation for the financial support of research at FSU (CHE-2102579). L.K. acknowledges support by the National Science Foundation Graduate Research Fellowship under Grant no. 1449440. Electron microscopy characterization was performed in the Department of Structural Studies of Zelinsky Institute of Organic Chemistry, Moscow.

■ DEDICATION

This work is dedicated to Professor I. P. Beletskaya, a pioneer in catalysis and transition metal chemistry on the occasion of her 90th birthday as a recognition of her many contributions as a scientist, a mentor, and a role model.

■ ABBREVIATIONS

TBHP, *tert*-butyl hydroperoxide; DTBP, di-*tert*-butyl peroxide; TFA, trifluoroacetic acid; NHPI, *N*-hydroxyphthalimide; TLC, thin layer chromatography

■ REFERENCES

- Standley, E. A.; Tasker, S. Z.; Jensen, K. L.; Jamison, T. F. Nickel Catalysis: Synergy between Method Development and Total Synthesis. *Acc. Chem. Res.* **2015**, *48*, 1503–1514.
- Wenger, O. S. Photoactive Nickel Complexes in Cross-Coupling Catalysis. *Chem.—Eur. J.* **2021**, *27*, 2270–2278.
- Guo, L.; Rueping, M. Decarbonylative Cross-Couplings: Nickel Catalyzed Functional Group Interconversion Strategies for the Construction of Complex Organic Molecules. *Acc. Chem. Res.* **2018**, *S1*, 1185–1195.
- Ananikov, V. P. Nickel: The “Spirited Horse” of Transition Metal Catalysis. *ACS Catal.* **2015**, *5*, 1964–1971.
- Arun, V.; Mahanty, K.; De Sarkar, S. Nickel-Catalyzed Dehydrogenative Couplings. *ChemCatChem* **2019**, *11*, 2243–2259.
- Diccianni, J.; Lin, Q.; Diao, T. Mechanisms of Nickel-Catalyzed Coupling Reactions and Applications in Alkene Functionalization. *Acc. Chem. Res.* **2020**, *53*, 906–919.
- Nebra, N. High-Valent NiIII and NiIV Species Relevant to C–C and C–Heteroatom Cross-Coupling Reactions: State of the Art. *Molecules* **2020**, *25*, 1141.
- Xu, H.; Diccianni, J. B.; Katigbak, J.; Hu, C.; Zhang, Y.; Diao, T. Bimetallic C–C Bond-Forming Reductive Elimination from Nickel. *J. Am. Chem. Soc.* **2016**, *138*, 4779–4786.
- Han, R.; Hillhouse, G. L. Carbon–Oxygen Reductive-Elimination from Nickel(II) Oxametallacycles and Factors That Control Formation of Ether, Aldehyde, Alcohol, or Ester Products. *J. Am. Chem. Soc.* **1997**, *119*, 8135–8136.
- Milbauer, M. W.; Kampf, J. W.; Sanford, M. S. Nickel(IV) Intermediates in Aminoquinoline-Directed C(sp²)–C(sp³) Coupling. *J. Am. Chem. Soc.* **2022**, *144*, 21030–21034.
- Camasso, N. M.; Sanford, M. S. Design, synthesis, and carbon–heteroatom coupling reactions of organometallic nickel(IV) complexes. *Science* **2015**, *347*, 1218–1220.
- Bour, J. R.; Ferguson, D. M.; McClain, E. J.; Kampf, J. W.; Sanford, M. S. Connecting Organometallic Ni(III) and Ni(IV): Reactions of Carbon-Centered Radicals with High-Valent Organonickel Complexes. *J. Am. Chem. Soc.* **2019**, *141*, 8914–8920.
- Roberts, C. C.; Chong, E.; Kampf, J. W.; Canty, A. J.; AriaFard, A.; Sanford, M. S. Nickel(II/IV) Manifold Enables Room-Temperature C(sp³)–H Functionalization. *J. Am. Chem. Soc.* **2019**, *141*, 19513–19520.
- Bour, J. R.; Camasso, N. M.; Sanford, M. S. Oxidation of Ni(II) to Ni(IV) with Aryl Electrophiles Enables Ni-Mediated Aryl–CF₃ Coupling. *J. Am. Chem. Soc.* **2015**, *137*, 8034–8037.
- Meucci, E. A.; Camasso, N. M.; Sanford, M. S. An Organometallic Ni(IV) Complex That Participates in Competing Transmetalation and C(sp²)–O Bond-Forming Reductive Elimination Reactions. *Organometallics* **2017**, *36*, 247–250.
- Ma, Z.; Mahmudov, K. T.; Aliyeva, V. A.; Gurbanov, A. V.; Guedes da Silva, M. F. C.; Pombeiro, A. J. L. Peroxides in metal complex catalysis. *Coord. Chem. Rev.* **2021**, *437*, 213859.
- Sosnovsky, G. Reactions of *t*-butyl peresters—III: Cuprous bromide-catalyzed reaction of peresters with ethers. *Tetrahedron* **1961**, *13*, 241–246.
- Hao, W.; Tian, J.; Li, W.; Shi, R.; Huang, Z.; Lei, A. Nickel-Catalyzed Oxidative C–H/N–H Isocyanide Insertion: An Efficient Synthesis of Iminoisoindolinone Derivatives. *Chem. - Asian J.* **2016**, *11*, 1664–1667.
- Li, Z.-l.; Wu, P.-y.; Sun, K.-k.; Cai, C. Nickel-catalyzed regioselective C–H acylation of chelating arenes: a new catalytic system for C–C bond formation via a radical process and its mechanistic explorations. *New J. Chem.* **2019**, *43*, 12152–12158.

(20) Doyle, M. P.; Patrie, W. J.; Williams, S. B. Nickel(II) bromide-catalyzed oxidations of primary and secondary alcohols to carbonyl compounds by benzoyl peroxide. *J. Org. Chem.* **1979**, *44*, 2955–2956.

(21) Paradis, P. M. Hydrogen Peroxide Bleaching of Amaranth Catalysed by Nickel(II) Nitrilotriacetic Acid. *Journal of Chemical Research* **1999**, *23*, 340–341.

(22) Bansal, V. K.; Thankachan, P. P.; Prasad, R. Catalytic and electrocatalytic wet oxidation of phenol using two new nickel(II) tetraazamacrocyclic complexes under heterogeneous conditions. *J. Mol. Catal. A: Chem.* **2010**, *316*, 131–138.

(23) Tang, S.; Wang, P.; Li, H.; Lei, A. Multimetallic catalysed radical oxidative C(sp³)–H/C(sp)–H cross-coupling between unactivated alkanes and terminal alkynes. *Nat. Commun.* **2016**, *7*, 11676.

(24) Qiu, Y.; Hartwig, J. F. Mechanism of Ni-Catalyzed Oxidations of Unactivated C(sp³)–H Bonds. *J. Am. Chem. Soc.* **2020**, *142*, 19239–19248.

(25) Kubo, T.; Chatani, N. Dicumyl Peroxide as a Methylating Reagent in the Ni-Catalyzed Methylation of Ortho C–H Bonds in Aromatic Amides. *Org. Lett.* **2016**, *18*, 1698–1701.

(26) Tsuzuki, S.; Sakurai, S.; Matsumoto, A.; Kano, T.; Maruoka, K. Ni-Catalyzed C(sp²)–H alkylation of N-quinolylbenzamides using alkylsilyl peroxides as structurally diverse alkyl sources. *Chem. Commun.* **2021**, *57*, 7942–7945.

(27) Chen, L.; Yang, J.-C.; Xu, P.; Zhang, J.-J.; Duan, X.-H.; Guo, L. N. Nickel-catalyzed Suzuki Coupling of Cycloalkyl Silyl Peroxides with Boronic Acids. *J. Org. Chem.* **2020**, *85*, 7515–7525.

(28) Li, Z.-L.; Cai, C. Pd/Ni catalyzed selective N–H/C–H methylation of amides by using peroxides as the methylating reagents via a radical process. *Org. Chem. Front.* **2017**, *4*, 2207–2210.

(29) Omer, H. M.; Liu, P. Computational Study of Ni-Catalyzed C–H Functionalization: Factors That Control the Competition of Oxidative Addition and Radical Pathways. *J. Am. Chem. Soc.* **2017**, *139*, 9909–9920.

(30) Vasilopoulos, A.; Krska, S. W.; Stahl, S. S. C(sp³)–H methylation enabled by peroxide photosensitization and Ni-mediated radical coupling. *Science* **2021**, *372*, 398–403.

(31) Parsaei, F.; Senarathna, M. C.; Kannangara, P. B.; Alexander, S. N.; Arche, P. D. E.; Welin, E. R. Radical philicity and its role in selective organic transformations. *Nat. Rev. Chem.* **2021**, *5*, 486–499.

(32) Zhao, R.; Fu, K.; Fang, Y.; Zhou, J.; Shi, L. Site-Specific C(sp³)–H Aminations of Imidates and Amidines Enabled by Covalently Tethered Distonic Radical Anions. *Angew. Chem., Int. Ed.* **2020**, *59*, 20682–20690.

(33) Liu, H.; Yu, J.-T.; Pan, C. Diacyl peroxides: practical reagents as aryl and alkyl radical sources. *Chem. Commun.* **2021**, *57*, 6707–6724.

(34) Kawamura, S.; Mukherjee, S.; Sodeoka, M. Recent advances in reactions using diacyl peroxides as sources of O- and C-functional groups. *Org. Biomol. Chem.* **2021**, *19*, 2096–2109.

(35) Ge, L.; Li, Y.; Jian, W.; Bao, H. Alkyl Esterification of Vinylarenes Enabled by Visible-Light-Induced Decarboxylation. *Chem.—Eur. J.* **2017**, *23*, 11767–11770.

(36) Zhao, R.; Chang, D.; Shi, L. Recent Advances in Cyclic Diacyl Peroxides: Reactivity and Selectivity Enhancement Brought by the Cyclic Structure. *Synthesis* **2017**, *49*, 3357–3365.

(37) Greene, F. D. Cyclic Diacyl Peroxides. I. Monomeric Phthaloyl Peroxide. *J. Am. Chem. Soc.* **1956**, *78*, 2246–2250.

(38) Greene, F. D. Cyclic Diacyl Peroxides. II. Reaction of Phthaloyl Peroxide with cis- and trans-Stilbene. *J. Am. Chem. Soc.* **1956**, *78*, 2250–2254.

(39) Greene, F. D.; Rees, W. W. Cyclic Diacyl Peroxides. III. The Reaction of Phthaloyl Peroxide with Olefins. *J. Am. Chem. Soc.* **1958**, *80*, 3432–3437.

(40) Adam, W.; Rucktaeschel, R. Photolysis and thermolysis of di-n-butylmalonyl peroxide. Evidence for α -lactone intermediates. *J. Org. Chem.* **1978**, *43*, 3886–3890.

(41) Adam, W.; Rucktaeschel, R. Cyclic peroxides. XVII. Solvolysis of dibutylmalonyl peroxide. *J. Org. Chem.* **1972**, *37*, 4128–4133.

(42) Griffith, J. C.; Jones, K. M.; Picon, S.; Rawling, M. J.; Kariuki, B. M.; Campbell, M.; Tomkinson, N. C. O. Alkene Syn Dihydroxylation with Malonyl Peroxides. *J. Am. Chem. Soc.* **2010**, *132*, 14409–14411.

(43) Rawling, M. J.; Tomkinson, N. C. O. Metal-free syndioxygenation of alkenes. *Org. Biomol. Chem.* **2013**, *11*, 1434–1440.

(44) Jones, K. M.; Tomkinson, N. C. O. Metal-Free Dihydroxylation of Alkenes using Cyclobutane Malonyl Peroxide. *J. Org. Chem.* **2012**, *77*, 921–928.

(45) Yuan, C.; Axelrod, A.; Varela, M.; Danysh, L.; Siegel, D. Synthesis and reaction of phthaloyl peroxide derivatives, potential organocatalysts for the stereospecific dihydroxylation of alkenes. *Tetrahedron Lett.* **2011**, *52*, 2540–2542.

(46) Yuan, C.; Liang, Y.; Hernandez, T.; Berriochoa, A.; Houk, K. N.; Siegel, D. Metal-free oxidation of aromatic carbon–hydrogen bonds through a reverse-rebound mechanism. *Nature* **2013**, *499*, 192.

(47) Eliasen, A. M.; Christy, M.; Claussen, K. R.; Besandre, R.; Thedford, R. P.; Siegel, D. Dearomatization Reactions Using Phthaloyl Peroxide. *Org. Lett.* **2015**, *17*, 4420–4423.

(48) Camelio, A. M.; Liang, Y.; Eliasen, A. M.; Johnson, T. C.; Yuan, C.; Schuppe, A. W.; Houk, K. N.; Siegel, D. Computational and Experimental Studies of Phthaloyl Peroxide-Mediated Hydroxylation of Arenes Yield a More Reactive Derivative, 4,5-Dichlorophthaloyl Peroxide. *J. Org. Chem.* **2015**, *80*, 8084–8095.

(49) Terent'ev, A. O.; Vil', V. A.; Gorlov, E. S.; Rusina, O. N.; Korlyukov, A. A.; Nikishin, G. I.; Adam, W. Selective Oxidative Coupling of 3H-Pyrazol-3-ones, Isoxazol-5(2H)-ones, Pyrazolidine-3,5-diones, and Barbituric Acids with Malonyl Peroxides: An Effective C–O Functionalization. *ChemistrySelect* **2017**, *2*, 3334–3341.

(50) Terent'ev, A. O.; Vil', V. A.; Gorlov, E. S.; Nikishin, G. I.; Pivnitsky, K. K.; Adam, W. Lanthanide-Catalyzed Oxyfunctionalization of 1,3-Diketones, Acetoacetic Esters, And Malonates by Oxidative C–O Coupling with Malonyl Peroxides. *J. Org. Chem.* **2016**, *81*, 810–823.

(51) Li, Y.; Ge, L.; Qian, B.; Babu, K. R.; Bao, H. Hydroalkylation of terminal aryl alkynes with alkyl diacyl peroxides. *Tetrahedron Lett.* **2016**, *57*, 5677–5680.

(52) Li, S.-L.; Wang, R.; Chen, J.; Zhang, H.; Hou, G.-K.; Lu, X.; Sun, Q.; Li, Y. Lewis Acid Catalyzed Three-Component Carbofunctionalization of Styrenes with Diacylperoxides and Nucleophiles. *Adv. Synth. Catal.* [online early access] **2023**, *365*, 17, .

(53) dos Passos Gomes, G.; Wimmer, A.; Smith, J. M.; Konig, B.; Alabugin, I. V. CO₂ or SO₂: Should It Stay, or Should It Go? *J. Org. Chem.* **2019**, *84*, 6232–6243.

(54) Kuhn, L.; Vil', V. A.; Barsegyan, Y. A.; Terent'ev, A. O.; Alabugin, I. V. Carboxylate as a Non-innocent L-Ligand: Computational and Experimental Search for Metal-Bound Carboxylate Radicals. *Org. Lett.* **2022**, *24*, 3817–3822.

(55) Wang, Q.; Zheng, H.; Chai, W.; Chen, D.; Zeng, X.; Fu, R.; Yuan, R. Copper catalyzed C–O bond formation via oxidative cross-coupling reaction of aldehydes and ethers. *Org. Biomol. Chem.* **2014**, *12*, 6549–6553.

(56) Raju, K. B.; Kumar, B. N.; Nagaiah, K. Copper-catalyzed acyloxylation of the C(sp³)–H bond adjacent to an oxygen by a cross-dehydrogenative coupling approach. *RSC Adv.* **2014**, *4*, 50795–50800.

(57) Wang, Q.; Geng, H.; Chai, W.; Zeng, X.; Xu, M.; Zhu, C.; Fu, R.; Yuan, R. Copper-Catalyzed Formation of C–O Bonds by Oxidative Coupling of Benzylic Alcohols with Ethers. *Eur. J. Org. Chem.* **2014**, *2014*, 6850–6853.

(58) Talukdar, D.; Borah, S.; Chaudhuri, M. K. Bis(acetylacetone)copper(II) catalyzed oxidative cross-dehydrogenative coupling (CDC) for the synthesis of α -acyloxy ethers through direct activation of α -C(sp³)–H bond of cyclic ether. *Tetrahedron Lett.* **2015**, *56*, 2555–2558.

(59) Priyadarshini, S.; Joseph, P. J. A.; Kantam, M. L. Copper catalyzed cross-coupling reactions of carboxylic acids: an expedient route to amides, 5-substituted γ -lactams and α -acyloxy esters. *RSC Adv.* **2013**, *3*, 18283–18287.

(60) Wang, H.-H.; Wen, W.-H.; Zou, H.-B.; Cheng, F.; Ali, A.; Shi, L.; Liu, H.-Y.; Chang, C.-K. Copper porphyrin catalyzed esterification of C(sp₃)-H via a cross-dehydrogenative coupling reaction. *New J. Chem.* **2017**, *41*, 3508–3514.

(61) Liu, Z.-Q.; Zhao, L.; Shang, X.; Cui, Z. Unexpected Copper-Catalyzed Aerobic Oxidative Cleavage of C(sp₃)-C(sp₃) Bond of Glycol Ethers. *Org. Lett.* **2012**, *14*, 3218–3221.

(62) Ghanbaripour, R.; Samadizadeh, M.; Honarpisheh, G.; Abdolmohammadi, M. Anchoring of a Copper(II)-Schiff Base Complex onto Silica-Coated Ferrite Nanoparticles: A Magnetically Separable Catalyst for Oxidative C–O Coupling by Direct C(sp₂)-H and C(sp₃)-H Bond Activation. *Synlett* **2015**, *26*, 2117–2120.

(63) Ha, P. T. M.; Le, T. D.; Doan, S. H.; Nguyen, T. T.; Le, N. T. H.; Phan, N. T. S. Synthesis of α -acyloxy ethers via direct esterification of carboxylic acids with ethers under metal-organic framework catalysis. *Tetrahedron* **2017**, *73*, 5883–5891.

(64) Wen, W.-H.; Xie, A.-N.; Wang, H.-H.; Zhang, D.-X.; Ali, A.; Ying, X.; Liu, H.-Y. Iron porphyrin-catalyzed C(SP3)-H activation for the formation of CO bond via cross-dehydrogenative coupling of cycloether and aromatic acid. *Tetrahedron* **2017**, *73*, 7169–7176.

(65) Zhao, J.; Fang, H.; Zhou, W.; Han, J.; Pan, Y. Iron-Catalyzed Cross-Dehydrogenative Coupling Esterification of Unactive C(sp₃)-H Bonds with Carboxylic Acids for the Synthesis of α -Acyloxy Ethers. *J. Org. Chem.* **2014**, *79*, 3847–3855.

(66) García-Cabeza, A. L.; Marín-Barrios, R.; Moreno-Dorado, F. J.; Ortega, M. J.; Vidal, H.; Gatica, J. M.; Massanet, G. M.; Guerra, F. M. Acyloxylation of 1,4-Dioxanes and 1,4-Dithianes Catalyzed by a Copper–Iron Mixed Oxide. *J. Org. Chem.* **2015**, *80*, 6814–6821.

(67) Lawesson, S.-O.; Berglund, C.; Gronwall, S.; Refn, S.; Andersen, V. K.; Jart, A. Studies on Peroxy Compounds. VIII. The Preparation of Acylals and Related Compounds by Copper Salt Catalyzed Reaction of t-Butyl Perbenzoate with Simple Ethers and Sulfides. *Acta Chem. Scand.* **1961**, *15*, 249–259.

(68) Ananikov, V. P.; Beletskaya, I. P. Toward the Ideal Catalyst: From Atomic Centers to a “Cocktail” of Catalysts. *Organometallics* **2012**, *31*, 1595–1604.

(69) Prima, D. O.; Kulikovskaya, N. S.; Galushko, A. S.; Mironenko, R. M.; Ananikov, V. P. Transition metal ‘cocktail’-type catalysis. *Curr. Opin. Green Sustain. Chem.* **2021**, *31*, 100502.

(70) Zima, A. M.; Lyakin, O. Y.; Ottenbacher, R. V.; Bryliakov, K. P.; Talsi, E. P. Dramatic Effect of Carboxylic Acid on the Electronic Structure of the Active Species in Fe(PDP)-Catalyzed Asymmetric Epoxidation. *ACS Catal.* **2016**, *6*, 5399–5404.

(71) Alabugin, I. V.; Bresch, S.; dos Passos Gomes, G. Orbital hybridization: a key electronic factor in control of structure and reactivity. *J. Phys. Org. Chem.* **2015**, *28*, 147–162.

(72) Alabugin, I. V.; Bresch, S.; Manoharan, M. Hybridization Trends for Main Group Elements and Expanding the Bent’s Rule Beyond Carbon: More than Electronegativity. *J. Phys. Chem. A* **2014**, *118*, 3663–3677.

(73) Luo, Y.-R. *Handbook of Bond Dissociation Energies in Organic Compounds*, 1st ed.; CRC Press: Boca Raton, 2002; p 392.

(74) Huang, X.; Liang, X.; Yuan, J.; Ni, Z.; Zhou, Y.; Pan, Y. Aerobic copper catalyzed α -oxyacetylation of ketones with carboxylic acids. *Org. Chem. Front.* **2017**, *4*, 163–169.

(75) Li, J.; Yang, Z.; Yang, T.; Yi, J.; Zhou, C. Copper-catalyzed α -C–H acyloxylation of carbonyl compounds with terminal alkynes. *New J. Chem.* **2018**, *42*, 1581–1584.

(76) Du, J.; Zhang, X.; Sun, X.; Wang, L. Copper-catalyzed direct α -ketoesterification of propiophenones with acetophenones via C-(sp₃)-H oxidative cross-coupling. *Chem. Commun.* **2015**, *51*, 4372–4375.

(77) Jia, W.-G.; Zhang, H.; Li, D.-D.; Yan, L.-Q. One-pot synthesis of acyloxy carbonyl compounds from ketones using a Pybox-copper(ii) catalyst. *RSC Adv.* **2016**, *6*, 27590–27593.

(78) Uyanik, M.; Suzuki, D.; Yasui, T.; Ishihara, K. In Situ Generated (Hypo)Iodite Catalysts for the Direct α -Oxyacetylation of Carbonyl Compounds with Carboxylic Acids. *Angew. Chem., Int. Ed.* **2011**, *50*, 5331–5334.

(79) Guo, S.; Yu, J.-T.; Dai, Q.; Yang, H.; Cheng, J. The Bu4NI-catalyzed alfa-acyloxylation of ketones with benzylic alcohols. *Chem. Commun.* **2014**, *50*, 6240–6242.

(80) Zhu, F.; Wang, Z.-X. Bu4NI-catalyzed α -acyloxylation reaction of ethers and ketones with aldehydes and tert-butyl hydroperoxide. *Tetrahedron* **2014**, *70*, 9819–9827.

(81) Mondal, B.; Sahoo, S. C.; Pan, S. C. nBu4NI-Catalyzed α -Benzoylation of Ketones with Terminal Aryl Alkenes. *Eur. J. Org. Chem.* **2015**, *2015*, 3135–3140.

(82) Li, C.; Jin, T.; Zhang, X.; Li, C.; Jia, X.; Li, J. Bu4NI-Catalyzed α -Oxyacetylation of Carbonyl Compounds with Toluene Derivatives. *Org. Lett.* **2016**, *18*, 1916–1919.

(83) Ochiai, M.; Takeuchi, Y.; Katayama, T.; Sueda, T.; Miyamoto, K. Iodobenzene-Catalyzed α -Acetoxylation of Ketones. In Situ Generation of Hypervalent (Diacyloxyido)benzenes Using m-Chloroperbenzoic Acid. *J. Am. Chem. Soc.* **2005**, *127*, 12244–12245.

(84) Beshara, C. S.; Hall, A.; Jenkins, R. L.; Jones, K. L.; Jones, T. C.; Killeen, N. M.; Taylor, P. H.; Thomas, S. P.; Tomkinson, N. C. O. A General Method for the α -Acyloxylation of Carbonyl Compounds. *Org. Lett.* **2005**, *7*, 5729–5732.

(85) Zhang, S.; Lian, F.; Xue, M.; Qin, T.; Li, L.; Zhang, X.; Xu, K. Electrocatalytic Dehydrogenative Esterification of Aliphatic Carboxylic Acids: Access to Bioactive Lactones. *Org. Lett.* **2017**, *19*, 6622–6625.

(86) Bityukov, O. V.; Matveeva, O. K.; Vil', V. A.; Kokorekin, V. A.; Nikishin, G. I.; Terent'ev, A. O. Electrochemically Induced Intermolecular Cross-Dehydrogenative C–O Coupling of β -Diketones and β -Ketoesters with Carboxylic Acids. *J. Org. Chem.* **2019**, *84*, 1448–1460.

(87) Vil', V. A.; Gorlov, E. S.; Bityukov, O. V.; Barsegyan, Y. A.; Romanova, Y. E.; Merkulova, V. M.; Terent'ev, A. O. C–O coupling of Malonyl Peroxides with Enol Ethers via [5 + 2] Cycloaddition: Non-Rubottom Oxidation. *Adv. Synth. Catal.* **2019**, *361*, 3173–3181.

(88) Vil', V. A.; Gorlov, E. S.; Shuingalieve, D. V.; Kunitsyn, A. Y.; Krivoshchapov, N. V.; Medvedev, M. G.; Alabugin, I. V.; Terent'ev, A. O. Activation of O-Electrophiles via Structural and Solvent Effects: SN2@O Reaction of Cyclic Diacyl Peroxides with Enol Acetates. *J. Org. Chem.* **2022**, *87*, 13980–13989.

(89) Vatsadze, S. Z.; Loginova, Y. D.; dos Passos Gomes, G.; Alabugin, I. V. Frontispiece: Stereoelectronic Chameleons: The Donor-Acceptor Dichotomy of Functional Groups. *Chem.—Eur. J.* **2017**, *23*, 3225–3245.

(90) Peterson, P. W.; Shevchenko, N.; Breiner, B.; Manoharan, M.; Lufti, F.; Delaune, J.; Kingsley, M.; Kovnir, K.; Alabugin, I. V. Orbital Crossings Activated through Electron Injection: Opening Communication between Orthogonal Orbitals in Anionic C1-C5 Cyclizations of Enediynes. *J. Am. Chem. Soc.* **2016**, *138*, 15617–15628.

(91) Davies, H. M. L.; Yang, J. Influence of a β -Alkoxy Substituent on the C–H Activation Chemistry of Alkyl Ethers. *Adv. Synth. Catal.* **2003**, *345*, 1133–1138.

(92) Babu, S. A.; Padmavathi, R.; Suwasia, S.; Dalal, A.; Bhattacharya, D.; Singh, P.; Tomar, R. Chapter 10 - Recent developments on the synthesis of functionalized carbohydrate/sugar derivatives involving the transition metal-catalyzed C–H activation/C–H functionalization. In *Studies in Natural Products Chemistry*, Attar, R., Ed.; Elsevier, 2021; Vol. 71, pp 311–399.

(93) Salamone, M.; Ortega, V. B.; Martin, T.; Bietti, M. Hydrogen Atom Transfer from Alkanols and Alkanediols to the Cumyloxy Radical: Kinetic Evaluation of the Contribution of α -C–H Activation and β -C–H Deactivation. *J. Org. Chem.* **2018**, *83*, 5539–5545.

(94) Giese, B.; González-Gómez, J. A.; Witzel, T. The Scope of Radical CC-Coupling by the “Tin Method. *Angew. Chem., Int. Ed.* **1984**, *23*, 69–70.

(95) Alabugin, I. V.; Kuhn, L.; Medvedev, M. G.; Krivoshchapov, N. V.; Vil', V. A.; Yaremenko, I. A.; Mehaffy, P.; Yarie, M.; Terent'ev, A. O.; Zolfogol, M. A. Stereoelectronic power of oxygen in control of chemical reactivity: the anomeric effect is not alone. *Chem. Soc. Rev.* **2021**, *50*, 10253–10345.

(96) Jo, T. G.; Klein, J. E. M. N. Gold-Catalyzed Direct C(sp₃)—H Acetoxylation of Saturated Hydrocarbons. *ChemCatChem*. **2021**, *13*, 4087–4091.

(97) Minisci, F.; Recupero, F.; Gambarotti, C.; Punta, C.; Paganelli, R. Selective functionalisation of hydrocarbons by nitric acid and aerobic oxidation catalysed by N-hydroxyphthalimide and iodine under mild conditions. *Tetrahedron Lett.* **2003**, *44*, 6919–6922.

(98) Moody, C. J.; O'Connell, J. L. Observations on the transition-metal catalysed oxidation of alkanes in trifluoroacetic acid: urea–hydrogen peroxide/TFA as a convenient method for the oxidation of unactivated C–H bonds. *Chem. Commun.* **2000**, 1311–1312.

(99) Zhou, J.; Jin, C.; Li, X.; Su, W. Copper-catalyzed oxidative esterification of unactivated C(sp₃)—H bonds with carboxylic acids via cross dehydrogenative coupling. *RSC Adv.* **2015**, *5*, 7232–7236.

(100) Bach, R. D.; Taaffee, T. H.; Holubka, J. W. Reaction of saturated organic compounds with acetyl and trifluoroacetyl nitrate. *J. Org. Chem.* **1980**, *45*, 3439–3442.

(101) Komiya, N.; Noji, S.; Murahashi, S.-I. Ruthenium-catalysed oxidation of alkanes with peracetic acid in trifluoroacetic acid: ruthenium as an efficient catalyst for the oxidation of unactivated C–H bonds. *Chem. Commun.* **2001**, 65–66.

(102) Coutard, N.; Goldberg, J. M.; Valle, H. U.; Cao, Y.; Jia, X.; Jeffrey, P. D.; Gunnoe, T. B.; Groves, J. T. Aerobic Partial Oxidation of Alkanes Using Photodriven Iron Catalysis. *Inorg. Chem.* **2022**, *61*, 759–766.

(103) Call, A.; Cianfanelli, M.; Besalú-Sala, P.; Olivo, G.; Palone, A.; Vicens, L.; Ribas, X.; Luis, J. M.; Bietti, M.; Costas, M. Carboxylic Acid Directed γ -Lactonization of Unactivated Primary C–H Bonds Catalyzed by Mn Complexes: Application to Stereoselective Natural Product Diversification. *J. Am. Chem. Soc.* **2022**, *144*, 19542–19558.

(104) Ottenbacher, R. V.; Bryliakova, A. A.; Shashkov, M. V.; Talsi, E. P.; Bryliakov, K. P. To Rebound or...Rebound? Evidence for the “Alternative Rebound” Mechanism in C–H Oxidations by the Systems Nonheme Mn Complex/H₂O₂/Carboxylic Acid. *ACS Catal.* **2021**, *11*, 5517–5524.

(105) Chen, X.-Y.; Yang, S.; Ren, B.-P.; Shi, L.; Lin, D.-Z.; Zhang, H.; Liu, H.-Y. Copper porphyrin-catalyzed cross dehydrogenative coupling of alkanes with carboxylic acids: Esterification and decarboxylation dual pathway. *Tetrahedron* **2021**, *96*, 132377.

(106) Zhao, J.; Fang, H.; Han, J.; Pan, Y. Cu-Catalyzed C(sp₃)—H Bond Activation Reaction for Direct Preparation of Cycloallyl Esters from Cycloalkanes and Aromatic Aldehydes. *Org. Lett.* **2014**, *16*, 2530–2533.

(107) Tran, B. L.; Driess, M.; Hartwig, J. F. Copper-Catalyzed Oxidative Dehydrogenative Carboxylation of Unactivated Alkanes to Allylic Esters via Alkenes. *J. Am. Chem. Soc.* **2014**, *136*, 17292–17301.

(108) Wang, C.-Y.; Song, R.-J.; Wei, W.-T.; Fan, J.-H.; Li, J.-H. Copper-catalyzed oxidative coupling of acids with alkanes involving dehydrogenation: facile access to allylic esters and alkylalkenes. *Chem. Commun.* **2015**, *51*, 2361–2363.

(109) Simmons, E. M.; Hartwig, J. F. On the Interpretation of Deuterium Kinetic Isotope Effects in C–H Bond Functionalizations by Transition-Metal Complexes. *Angew. Chem., Int. Ed.* **2012**, *51*, 3066–3072.

(110) Yaremenko, I. A.; Belyakova, Y. Y.; Radulov, P. S.; Novikov, R. A.; Medvedev, M. G.; Krivoshchapov, N. V.; Korlyukov, A. A.; Alabugin, I. V.; Terent'ev, A. O. Inverse α -Effect as the Ariadne's Thread on the Way to Tricyclic Aminoperoxides: Avoiding Thermodynamic Traps in the Labyrinth of Possibilities. *J. Am. Chem. Soc.* **2022**, *144*, 7264–7282.

(111) Yaremenko, I. A.; Belyakova, Y. Y.; Radulov, P. S.; Novikov, R. A.; Medvedev, M. G.; Krivoshchapov, N. V.; Alabugin, I. V.; Terent'ev, A. O. Cascade Assembly of Bridged N-Substituted Azaozonides: The Counterintuitive Role of Nitrogen Source Nucleophilicity. *Org. Lett.* **2022**, *24*, 6582–6587.

(112) Vil', V. A.; Barsegyan, Y. A.; Barsukov, D. V.; Korlyukov, A. A.; Alabugin, I. V.; Terent'ev, A. O. Peroxycarbonium Ions as the “Gatekeeper” in Reaction Design: Assistance from Inverse Alpha-Effect in Three-Component β -Alkoxy- β -peroxy lactones Synthesis. *Chem.—Eur. J.* **2019**, *25*, 14460–14468.

(113) Vil', V. A.; dos Passos Gomes, G.; Bityukov, O. V.; Lyssenko, K. A.; Nikishin, G. I.; Alabugin, I. V.; Terent'ev, A. O. Interrupted Baeyer–Villiger Rearrangement: Building A Stereoelectronic Trap for the Criegee Intermediate. *Angew. Chem., Int. Ed.* **2018**, *57*, 3372–3376.

(114) Yaremenko, I. A.; Belyakova, Y. Y.; Radulov, P. S.; Novikov, R. A.; Medvedev, M. G.; Krivoshchapov, N. V.; Korlyukov, A. A.; Alabugin, I. V.; Terent'ev, A. O. Marriage of Peroxides and Nitrogen Heterocycles: Selective Three-Component Assembly, Peroxide-Preserving Rearrangement, and Stereoelectronic Source of Unusual Stability of Bridged Azaozonides. *J. Am. Chem. Soc.* **2021**, *143*, 6634–6648.

(115) Vil', V. A.; Barsegyan, Y. A.; Kuhn, L.; Ekimova, M. V.; Semenov, E. A.; Korlyukov, A. A.; Terent'ev, A. O.; Alabugin, I. V. Synthesis of unstrained Criegee intermediates: inverse α -effect and other protective stereoelectronic forces can stop Baeyer–Villiger rearrangement of γ -hydroperoxy- γ -peroxy lactones. *Chem. Sci.* **2020**, *11*, 5313–5322.